domain, the method followed by Tetsumoto et al. is attractive as it offers a substantial simplification of the apparatus. For example, dealing with the carrier envelop offset frequency of the comb is not necessary. The record low phase noise eventually realized at 300 GHz — already challenging to achieve and characterize — shows clearly that the cost in terms of ultimate performance induced by this approach is largely offset by the increased simplicity of the experimental demonstration.

Once the phase-locking of the DKS comb is realized, the 300 GHz signal is still virtual, in that it is encoded in the repetition rate of the optical pulses from the comb. It is then necessary to generate from the virtual signal a 'real' 300 GHz electromagnetic wave and, most importantly, characterize its phase noise. The use of a special, very high bandwidth, uni-travelling-carrier photodiode (UTC-PD) makes the first part possible, as it allows generation of the 300 GHz wave by direct photodetection of the pulse train emitted by the DKS comb.

The phase noise characterization at the required level is particularly challenging in this frequency range and Tetsumoto et al. combine three different techniques to make it possible. This approach allows different parts of the Fourier frequencies spectrum to be targeted with the most appropriate of the three techniques (that is, the one that exhibits the lowest noise floor readout). It also increases the general trust in the measurement, since, as expected, the different techniques give the same results at the few places in the Fourier spectrum where they are not limited by their readout noise.

These three techniques rely on comparing the DKS-comb-generated 300 GHz signal with a signal from a classic optoelectronic source, realized by multiplying the frequency of a low noise microwave source at 10 GHz (a dielectric resonant oscillator (DRO)) to 300 GHz by high-modulation-index optical phase modulation of a mid-infrared optical carrier. Depending on the part of the Fourier spectrum of interest, this classic source can be free-running, and used directly as a low-noise reference (for high Fourier frequencies) or phase-locked to the 300 GHz, so that the 10 GHz DRO signal itself copies the spectral purity of the 300 GHz source (but divided by 30), and can be used for analysing its phase noise with conventional instrumentation (for low Fourier frequencies). However, in the intermediate frequency range (8–50 kHz), the authors had to use a more exotic approach, where the DRO signal is analysed by a low-noise homemade two-wave delay-line interferometer, which is, roughly speaking, a special and highly optimized implementation of the self-interferometry technique with a long delay line.

The final phase noise estimation, realized by stitching the results from the three measurement methods, exhibits a record low phase (or equivalently timing) noise for a 300 GHz source, with a value substantially below 10 as $Hz^{-1/2}$ from Fourier frequencies above 10 kHz from the carrier.

This achievement is an important milestone as it demonstrates the usefulness of the ultra-compact DKS comb approach for the generation of low-phase-noise signals at the higher end of the millimetre-wave band (close to the terahertz band). In this region, classic optical frequency comb systems with a repetition rate typically in the radio-frequency domain are difficult or impossible to use, even with the help of pulse–interleaver-based frequency multiplication systems[9].

Furthermore, the integrated-photonic nature of the DKS comb holds promises for the ultimate goal of development of a fully integrated, compact source of a low-phase-noise signal in the millimetre range. Of course, there is still a long way to go between the work of Tetsumoto et al. and a fully integrated-photonic turn-key system that is easily field-deployable in applications such as a future communications system, for example. Beyond the DKS comb itself, many other components will have to be integrated as well. However, this latest achievement is certainly paving the way towards such a bright future where low-noise sources throughout the millimetre range could be available in a compact and easy-to-use manner. ❐

Yann Le Coq
LNE-SYRTE, Observatoire de Paris, Université PSL, CNRS, Sorbonne Université, Paris, France.
✉*e-mail: yann.lecoq@obspm.fr*

Published online: 1 July 2021
https://doi.org/10.1038/s41566-021-00838-3

References

1. Hati, A. et al. *IEEE Trans. Ultrason. Ferroelectr. Freq. Control* **60**, 1796–1803 (2013).
2. Xie, X. et al. *Nat. Photon.* **11**, 44–47 (2017).
3. Argence, B. et al. *Nat. Photon.* **9**, 456–460 (2015).
4. Pupeza, I., Zhang, C., Högner, M. & Ye, J. *Nat. Photon.* **15**, 175–186 (2021).
5. Kippenberg, T. J., Gaeta, A. L., Lipson, M. & Gorodetsky, M. L. *Science* **361**, eaan8083 (2018).
6. Liu, J. et al. *Nat. Photon.* **14**, 486–491 (2020).
7. Lucas, E. et al. *Nat. Commun.* **11**, 374 (2020).
8. Tetsumoto, T. et al. *Nat. Photon.* https://doi.org/10.1038/s41566-021-00790-2 (2021).
9. Haboucha, A. et al. *Opt. Lett.* **36**, 3654–3656 (2011).

Competing interests

The author declares no competing interests.

Check for updates

GRAPHENE PHOTONICS

Chameleon graphene surfaces

The unique optical properties of graphene were combined with lithium-ion battery technology to produce multispectral optical devices, with colour-changing capabilities.

Andrea C. Ferrari

Graphene is an ideal material for photonics and optoelectronics, where the combination of its unique optical and electronic properties can be fully exploited[1]. Graphene is gapless. This enables charge carrier generation by light absorption over a very wide energy spectrum, unmatched by other materials. This includes the ultraviolet, visible, short-wave infrared, near-infrared, mid-infrared, far-infrared and terahertz (THz). Furthermore, graphene exhibits ultrafast carrier dynamics[2], wavelength-independent absorption[3], tunable optical properties via change of its chemical potential/Fermi level[4], E_F, low dissipation

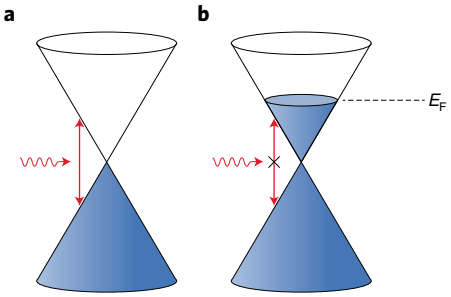

Fig. 1 | Basic principle of light interaction with doped graphene. a,**b**, If the incident photon energy is larger than $2E_F$, light can be absorbed (**a**); otherwise, light absorption is blocked (**b**).

rates and high mobility[5]. The reference E_F = 0 eV is conventionally taken to be at the Dirac point, that is, the intersection of the two cones representing the conduction and valence bands of single-layer graphene (SLG) (Fig. 1). The Fermi energy coincides with E_F at 0 K. For electrostatic doping, at room temperature, it is common to approximate E_F ≈ Fermi energy.

The ability to tune the optical response of a material via electrostatic gating is crucial for optoelectronic applications, such as electro-optic modulators, saturable absorbers for mode-locking of a variety of ultrafast and broadband lasers, optical limiters, photodetectors and transparent electrodes[1]. The SLG band structure, with zero gap, linearly dispersive conduction and valence bands (Fig. 1) enables an easy control of E_F and of the threshold for interband optical absorption, with ultra-wide-band tunability[4], as well as gate-controllable third-harmonic enhancement[6], paving the way for electrically tunable broadband frequency converters for optical communications and signal processing.

Many of the characteristics and unique capabilities of SLG-based photonic and optoelectronic systems have been studied, and several applications addressed[1,7,8]. Graphene-integrated photonics is an emerging platform for wafer-scale manufacturing of modulators, detectors and switches for next-generation datacom and telecom[7,8].

In SLG, absorption and refractive index depend on E_F and the intraband and interband transitions of electrons and holes excited by impinging photons[9]. In undoped SLG, the absorption of photons of any wavelength is allowed[3]. However, if E_F is increased above half the photon energy, because of Pauli blocking, carrier excitation is inhibited, and SLG becomes transparent[10] (Fig. 1). Electro-absorption modulation in SLG can be achieved by E_F modulation[11]. This also causes phase modulation, because absorption and refractive index depend on E_F (ref. [12]). When interband transitions are inhibited, absorption can occur as a result of intraband transitions. These are primarily a consequence of long-range scattering induced by, for example, impurities, trap states and screening. A convenient way of describing the overall effect of intraband transitions is the scattering time τ. The longer the τ, the lower the intraband absorption, which means the more transparent SLG becomes in the E_F range where interband transitions are excluded because of Pauli blocking.

Conventional optoelectronic devices, such as light sources and detectors, are usually designed to operate at certain wavelengths to obtain the highest efficiency. New opportunities open up for multi-spectral devices working over wavelengths and optical photon energies differing by orders of magnitude. These require broadband electro-optical tunability, multispectral device structure and non-volatile switching. Phase-change[13] and electrochromic materials[14] are capable of colour change triggered by temperature or electric field, but they require a conductive top electrode, potentially limiting their spectral range.

Reporting in *Nature Photonics*, Muhammed Said Ergoktas and colleagues present several graphene-based electro-optical devices, with multispectral tuning from visible to microwave[15]. They realized these based on electrochemistry, with reversible lithium (Li) intercalation between the sheets of multi-layer graphene (MLG). The state of charge of the constituent electrochemical cells is used to modulate the spectral intensity in different wavelength ranges, with a new device concept linking electrochemistry with tuning of optical properties. MLG is prepared by chemical vapour deposition on nickel foils, ideal for MLG growth, unlike copper, which is more suitable for SLG[16]. The roll-to roll process used by Ergoktas and colleagues is also scalable to large areas. A MLG with ~150 layers is used as anode, with an aluminium foil coated with Li-doped nickel manganese cobalt oxide as cathode. This architecture bears close resemblance to that of Li-ion batteries. As in batteries, the Li ions intercalate into MLG, thus modulating E_F of each layer[15]. For this reason, even if the non-intercalated cathode is a MLG, the relevant physics ruling the device optical properties is that of SLG, as described above, since the layers are decoupled by the Li intercalation process.

Being electrochemical in nature, these devices cannot compete with the modulation speed of electrically or optically tuned photodetectors or modulators[1,4,7,8,11]. Ergoktas and colleagues showed that their devices can be turned on/off within ~1 s in the THz range, ~3 s in the infrared, and tens of seconds in the visible. These speeds are consistent with the amount of charge required to modify the optical response in the respective regimes. As the optical response is linked to the amount of charge, the response time scales with the device current. Thus, it could be scaled by a factor ~10 by increasing the charging current by the same amount. Ergoktas and colleagues prioritized the long-term operation stability by keeping the device current at a level similar to that of Li-ion batteries (~1 mA cm^{-2}).

These speeds are not as fast as those needed for display applications, such as those exploiting liquid crystals or organic light-emitting diodes. Thus, the team suggested other uses, such as tunable solar reflectors for space applications. A 10–40 s response time in the visible is acceptable for dynamic thermal regulation of a satellite, since this is much faster than the typical orbital periods, even for low-orbit satellites. Applications that require tunable infrared emissivity include thermal camouflage and radiative heat transport, both demonstrated by Ergoktas and colleagues. For thermal camouflaging, the switching speeds are dictated by the changes in the background. For a stationary or slowly moving object, the background varies within a day, as the ambient temperature fluctuates, or clouds move. In this case, the response time is sufficient. For a fast target, such as a vehicle moving in a terrain with non-uniform temperature, the background can change within seconds. This would limit the use of the technology reported by Ergoktas and colleagues in its current state, thus requiring improvements to its transient response, such as optimizing it just for the infrared.

As for any other electrochemical devices, cyclability is one of the main concerns. Ergoktas and colleagues tested the endurance in THz, infrared and visible ranges, showing that the devices can operate for over 11,000, 2,200 and 580 on/off cycles in these regimes, respectively. Interestingly, due to the similarity of architecture, they also showcased the use of this new technology as charge level indicator for Li-ion pouch cell batteries.

These new multispectral electro-optical devices, operating over the entire electromagnetic spectrum from the visible to microwave, could inspire new technologies for tunable optics, either as standalone

units, or incorporated with established light manipulation approaches. Combining these devices with the broad electro-optical tunability of SLG's plasma frequency may yield electrically tunable plasmonic systems, which would enable multispectral active plasmonics.

The exploitation of electrochemistry to tune SLG's optical properties stimulates a new promising direction of research for this unique material. In principle, other layered materials could also be investigated by adapting the approach presented by Ergoktas and colleagues. Vice versa, key aspects of Li-ion battery performance can be studied by investigating the changes in the optical and spectroscopic properties occurring during intercalation and de-intercalation of graphitic anodes, to unravel the signatures of Li-ion induced doping, staging and degradation upon cycling. This could lead to a better understanding of the battery degradation processes. Li intercalation/de-intercalation may cause changes in graphite or silicon–graphite anodes in different cycles, affecting battery cycling performance. The unique physics of light–matter interaction in SLG will be the basis to develop optical-based diagnostic tools to improve control and prediction of the state of health of batteries. ❐

Andrea C. Ferrari ✉
Cambridge Graphene Centre, University of Cambridge, Cambridge, UK.
✉*e-mail: acf26@eng.cam.ac.uk*

Published online: 16 June 2021
https://doi.org/10.1038/s41566-021-00839-2

References

1. Bonaccorso, F., Sun, Z., Hasan, T. & Ferrari, A. C. *Nat. Photon.* **4**, 611–622 (2010).
2. Brida, D. et al. *Nat. Commun.* **4**, 1987 (2013).
3. Nair, R. R. et al. *Science* **320**, 1308 (2008).
4. Wang, F. et al. *Science* **320**, 206–209 (2008).
5. Mayorov, A. S. et al. *Nano Lett.* **11**, 2396–2399 (2011).
6. Soavi, G. et al. *Nat. Nanotechnol.* **13**, 583–588 (2018).
7. Koppens, F. H. L. et al. *Nat. Nanotechnol.* **9**, 780–793 (2014).
8. Romagnoli, M. et al. *Nat. Rev. Mater.* **3**, 392–414 (2018).
9. Stauber, T., Peres, M. N. R. & Geim, A. K. *Phys. Rev. B* **78**, 085432 (2008).
10. Mak, K. F., Ju, L., Wang, F. & Heinz, T. F. *Solid State Commun.* **152**, 1341–1349 (2012).
11. Liu, M. *Nature* **474**, 64–67 (2011).
12. Chang, Y.-C., Liu, C.-H., Liu, C.-H., Zhong, Z. & Norris, T. B. *Appl. Phys. Lett.* **104**, 261909 (2014).
13. Wuttig, M., Bhaskaran, H. & TAubner, T. *Nat. Photon.* **11**, 465–476 (2017).
14. Granqvist, C. G. et al. *Electrochim. Acta* **259**, 1170–1182 (2018).
15. Ergoktas, M. S. et al. *Nat. Photon.* https://doi.org/10.1038/s41566-021-00791-1 (2021).
16. Backes, C. et al. *2D Mater.* **7**, 022001 (2020).

Competing interests

The author declares no competing interests.

Check for updates

X-RAY PHOTONICS

Transient gratings with X-rays

Short period, femtosecond transient gratings in a sample can now be produced by X-rays. The approach promises to reveal the excitation behaviour of complex materials with high temporal and spatial resolution.

Martin Beye

X-ray free-electron lasers (XFELs) — a handful of large-scale facilities worldwide, the first being in operation for experimentalists for over a decade and more just starting — have opened new avenues for X-ray science[1]. They produce ultrashort and intense X-ray pulses that are able to access atomic length and timescales (that is, subnanometre and femtosecond). This capability makes it possible to study electron and nuclear dynamics as they occur, for example, in photo-induced reactions where this information is important to understand and optimize solar energy conversion.

Most operational XFELs are based on the process of self-amplified spontaneous emission (SASE) that generates pulses with high spatial (transverse) coherence but poor temporal (longitudinal) coherence. With monochromatization downstream or inside the light amplification chain (the latter termed self-seeding) or with external seeding by an optical laser, full longitudinal coherence can be generated and the X-ray pulses gain all properties of laser light[2].

Developments are ongoing to also adapt advanced experimental techniques, like wave-mixing methods — well-known from optical lasers — to the X-ray region. The simplest processes for combining several interactions of a system with X-ray photons are, for example, harmonic generation or stimulated emission. Several observations have been reported, but the short lifetime of the core-excited state, often shorter than the available pulse durations as well as the occurrence of concurrent X-ray-induced processes limit experimental observation[3].

More evolved wave-mixing techniques can make use of beams coming from several directions in so-called phase-matching geometries. Such schemes produce unique signals emitted into new directions, where no other beams appear[4]. These techniques require the spatial and temporal overlap of several X-ray beams from different distinct directions. Progress has been hindered largely because of the absence of simple beam manipulation devices for X-rays. Beam focusing and steering of X-rays is not simple, requiring super-polished high-quality grazing incidence mirrors (with deflection angles often below a handful of degrees), or Bragg reflections from crystals for fixed wavelengths.

The main missing piece of equipment is a simple amplitude beam splitter, a function that can be easily realized in the optical regime with a piece of coated glass. For X-rays though the options are limited: one possible method is the use of thin Bragg crystals, which reflect a spectrally selected portion of the beam while transmitting the remaining part. But this does not normally result in a simple amplitude division[5] and this approach also has potential production, handling and stability issues.

More recently, the use of nanostructured transmission gratings has been explored to split X-ray beams, where the negative and positive diffraction orders of the grating produce a pair of identical copies of the beam[6]. The recombination of these beams onto a sample is not easily realized, though, and typically requires another set of precisely controlled optical elements[7].

Now, writing in *Nature Photonics*, Rouxel et al.[8] show that this set of optical elements